Organic supramolecular room-temperature phosphorescence featuring profound dependence on host-guest binding behaviors

Chunhui Li
East China University of Science and Technology
Qichao Guo
East China University of Science and Technology
Jinkang Zhu
East China University of Science and Technology
Qiaochun Wang (qcwang@ecust.edu.cn)
East China University of Science and Technology

Research Article

Keywords: Cucurbit[n]uril, Supramolecular, Phosphorescence, Binding constant, Job's plot, Nonlinear least-squares curve-fitting

Posted Date: February 14th, 2023

DOI: https://doi.org/10.21203/rs.3.rs-2567169/v1

Abstract

Recent years have witnessed tremendous progresses in the field of cucurbit[n]uril (CB[n])-based organic supramolecular room-temperature phosphorescence (RTP). However, the relationship between phosphorescence property and host-guest binding behaviors has been ignored in this research area. Herein, three guest compounds (G1, G2 and G3), featuring a same luminescence core (4-(4-bromophenyl)-1-methylpyridinium chloride) and the relatively similar molecular phosphorescence properties, can form 1:1 complexes with phCB[6] respectively in an order of descending enwrapping degrees (phCB[6]/G1 > phCB[6]/G2 > phCB[6]/G3), along with which The RTP quantum yields of these three supramolecular complexes in solid state show a distinctly decreasing trend, thereby demonstrating an obvious influence of host-guest binding behaviors on phosphorescence performance. This work may provide a new idea for the design of high-performance RTP materials.

1. Introduction

The research of organic RTP has attracted increasing attention in recent years due to its promising application prospect, such as information encryption and anti-counterfeiting[1], time-resolved bio-imaging[2], display[3], sensors[4], detection[5], and so forth. However, organic compounds generally emit no or weak RTP owning to its inherent weak intersystem crossing (ISC) efficiency and the lack of rigid internal environment[6]. To date, various effective strategies have been proposed to activate or improve the RTP performance for organic compounds, including H-aggregation[7], intermolecular and intramolecular halogen bond[8, 9], intermolecular electron coupling[10], host-guest doping[11–14], polymer assistance[15, 16] and supramolecular strategy[17].

Among the above strategies, supramolecular strategy is now a hotspot, which mainly takes advantage of the host-guest binding[18, 19]. A host such as a cyclodextrin or CB[n] can enwrap an organic luminescent guest by the hydrophobic cavity and provide a rigid and isolated microenvironment for every guest molecule, which can not only restrict the molecular motion, but also prevent aggregation-caused quenching and shield oxygen, thereby activating the RTP[17, 20]. For example, an RTP aqueous solution has been realized by Ma and Tian in 2019 by utilizing the self-assembling between triazine derivative and CB[8][21]. Liu's group has raised a concept of "macrocycles enhance guest's phosphorescence"[22] and a serious of ultra-highly efficient supramolecular RTP systems have been constructed on this basis[20, 23–28]. It is believed that supramolecular RTP will turn into a new growth point in the realm of RTP.

As compared to the too much focus on high RTP performance, little attention has been paid to the investigation of the relationship between supramolecular RTP property and host-guest binding behaviors. How does the degree of inclusion affect the phosphorescence performance? Herein, three guest compounds (G1, G2 and G3) were used to construct supramolecular RTP systems with phCB[6] - a monophenyl functionalized CB[6][29], which is characterized by fine water solubility and ellipsoidal deformation (Scheme 1). The three guests share a same luminescent core, 4-(4-bromophenyl)-1-methylpyridinium chloride, thereby having relatively similar phosphorescence efficiency ranging from

13.5–20.1% in molecule state. In contrast, after enwrapped by phCB[6], the three formed 1:1 host-guest complexes exhibit totally distinct RTP quantum yields of 78%, 36% and 18% for phCB[6]/G1, phCB[6]/G2 and phCB[6]/G3 respectively in solid state, for the reason of the descending degrees of inclusion. It is envisaged that this work could provide a new design idea for constructing high-performance supramolecular RTP materials.

2. Experiment

2.1 General information

^{1}H NMR and ^{1}H–^{1}H COSY spectra were recorded on a Bruker AV-400 spectrometer. The matrix-assisted laser desorption ionization - time of flight mass spectrometry (MALDI-TOF MS) was performed on a 4800 Plus M-TOF/TOF analyzer (AB SCIEX, USA) and a LCT Premier XE mass spectrometer. The HPLC was performed using Agilent 1260 with analytical Sunniest C18 column (4.6 mm × 250 mm). The UV–Vis absorption spectra were obtained on a Varian Cary 100 spectrometer and a Varian Cary Eclipse (1 cm quartz cell was used). The photoluminescence spectra and lifetimes were measured on Edinburgh FLS920 instrument. The absolute phosphorescence quantum yields were achieved by using an integrating sphere on a HAMAMATSU Quantaurus QY C11347-1.

2.2 Synthesis

The synthetic routes of phCB[6] and three guests were shown in Scheme 2. The synthetic procedures were described underneath their corresponding ^{1}H NMR spectra in supporting information. HPLC measurements were performed to guarantee their structures and purity to eliminate the interference from impurity (Fig. S8-S10). The glycoluril, phthaladehyde, pyridin-4-ylboronic acid, 1-bromo-4-iodo-2-methylbenzene and 2-bromo-5-iodo-1,3-dimethylbenzene were commercially available and have been purified by column chromatography and recrystallization before used.

2.2.1 6C (Fig. S1)

^{1}H NMR (400 MHz, D_2O, > 1.0 equiv. p-xylylenediammonium hydrochloride (PXDA·2HCl) was added): δ 7.40 (s, 1.78H, unbound PXDA·2HCl), 6.60 (s, 4H, bound PXDA·2HCl), 5.72 (d, *J* = 15.6 Hz, 2H), 5.60–5.38 (m, 16H), 5.30 (q, *J* = 8.9 Hz, 4H), 4.31 (d, *J* = 15.6 Hz, 2H), 4.12 (d, *J* = 15.6 Hz, 5.87H, including 1.87H of unbound PXDA·2HCl), 4.02 (d, *J* = 15.6 Hz, 8H, including 4H of bound PXDA·2HCl).

2.2.2 phCB[6] (Fig. S2 and S3)

^{1}H NMR (400 MHz, D_2O, 298K, 1.0 equiv. PXDA·2HCl was added): δ 7.61 (s, 4H), 7.39 (s, 2H, unbound probe), 6.77 (s, 2H), 6.43 (s, 4H, bound probe), 5.80 (d, *J* = 16 Hz, 2H), 5.63 (d, *J* = 8.8 Hz, 2H), 5.50 (m, 10H), 5.19 (d, *J* = 9.2 Hz, 2H), 5.10 (d, *J* = 8.8 Hz, 2H), 5.00 (d, *J* = 9.6 Hz, 2H), 4.81 (d, *J* = 9.6 Hz, 2H), 4.47 (d, *J* = 16 Hz, 2H), 4.30 (s, 4H, bound probe), 4.13–4.03 (m, 6H, including 2H of unbound probe), 3.89 (d, *J*

= 15.2 Hz, 4H). HRMS (ESI) Found: $[M + PXDA{\cdot}2HCl - 2Cl]^{2+}$ 604.2128; molecular formula $C_{42}H_{38}N_{24}O_{12}{\cdot}C_8H_{14}N_2Cl_2$ requires $[M + PXDA{\cdot}2HCl - 2Cl]^{2+}$ 604.2124.

2.2.3 P2 (Fig. S4)

^{1}H NMR (400 MHz, $CDCl_3$, 298K): δ 8.67 (d, *J* = 6.0 Hz, 2H), 7.66 (d, *J* = 8.0 Hz, 2H), 6.77 (s, 2H), 7.50 (m, 3H), 7.33 (dd, *J* = 8.0 and 2.0 Hz, 1H), 2.50 (s, 3H).

2.2.4 P3 (Fig. S5)

^{1}H NMR (400 MHz, $CDCl_3$, 298K): δ 8.65 (d, *J* = 4.4 Hz, 2H), 7.50 (d, *J* = 4.4 Hz, 2H), 7.34 (s, 2H), 2.50 (s, 6H).

2.2.5 G2 (Fig. S6)

^{1}H NMR (400 MHz, D_2O, 298K): δ 8.59 (d, *J* = 6.8 Hz, 2H), 8.00 (d, *J* = 6.8 Hz, 2H), 7.57 (d, *J* = 2.0 Hz, 1H), 7.52 (d, *J* = 8.4 Hz, 1H), 7.37 (dd, *J* = 8.4 and 2.0 Hz, 1H), 4.22 (s, 3H), 2.25 (s, 3H).

2.2.6 G3 (Fig. S7)

^{1}H NMR (400 MHz, D_2O, 298K): δ 8.56 (d, *J* = 6.8 Hz, 2H), 7.90 (d, *J* = 6.8 Hz, 2H), 7.32 (s, 2H), 4.21 (s, 3H), 2.19 (s, 6H).

3. Results And Discussions

Our previous work has proved that G1 and phCB[6] can form a highly encapsulated host-guest complex[30] with the whole pyridinium unit and part of the benzene ring of G1 entering into the host cavity (Scheme 1). In this work, one (G2) and two (G3) methyl were introduced onto the ortho-position of C-Br bond on G1 skeleton respectively, with an aim to regulate the depth of skeleton into the cavity of phCB[6] by the steric hindrance, so as to achieve host-guest complexes with different enwrapping degrees and explore its influence on supramolecular RTP performance. Due to the weak electron-donating ability and long distance away from pyridine unit, methyl was adopted to reduce the influence on the π-electron distribution of the guest backbone, thereby ensuring that the three guests exhibit similar photophysical properties in molecule state.

3.1 The photophysical properties of the three guests in solution state (including water and methanol) at RT

The three guests were prepared and their photophysical properties in diluted aqueous solution (2×10^{-5} mol/L) were then investigated. The absorption and photoluminescence (PL) spectra (Fig. S11) of the three guests show slight bathochromic shifts (λmax abs at 303, 307 and 310 nm for absorption, and λmax PL at 380, 390 and 400 nm for PL, respectively) with the increasing number of the methyl substituents, verifying that the weak electron-donating nature of the methyl group has relative weak impact on the photophysical properties of these guests. Furthermore, the photophysical properties of the

three guests in methanol solution (2×10^{-5} mol/L) are basically identical to those in aqueous solution (Fig. 1a and Fig. S12a), indicating no intramolecular charge transfer character for the three guests. The time-resolved PL decay curves show nanosecond-level lifetimes (0.15, 0.16 and 0.56 ns) for the three emission maximums in methanol (Fig. S12b-12d), which demonstrates that there is no phosphorescence emission in solution state for all the guests because of drastic non-radiative triplet dissipation.

3.2 The photophysical properties of the three guests in methanol at 77K

Further photophysical measurements of above methanol solutions were carried out at cryogenic temperature (77 K) to activate the phosphorescence (Fig. 1b-1d). In the PL spectrum of G1, there are two emission bands with maximums at approximate 350 and 495 nm respectively. The delayed (0.5 ms) PL spectrum exhibits only one emission band and overlaps with the latter emission band in PL spectrum, thereby implying a phosphorescence nature for 495 nm. Subsequent fitted lifetimes can adequately ascribe 350 nm (1.1 ns) and 495 nm (20.1 ms) to be fluorescence and phosphorescence emission respectively (Fig. S13a and 13b). The dual emission peaks share a same excitation band with a maximum at 300 nm, demonstrating that the fluorescence and phosphorescence come from a same luminescent backbone. It is worth noting that the fluorescence band at 77 K displays a hypochromatic shift of 30 nm as compared to that at RT, which is a common phenomenon at cryogenic condition in previous reports due to the confined molecular conformation[8, 31]. With regard to G2 and G3 (Fig. 1c and 1d), their PL spectra both basically show one emission band located at a maximum of 500 nm. The delayed (0.5 ms) PL spectra and lifetimes can clearly prove its phosphorescence nature (Fig. S13c and S13d), which meantime demonstrates that G2 and G3 have the similar triplet energy with G1 in molecular state.

3.3 The photophysical properties of the three guests in film state at RT

The phosphorescence efficiency at RT of the three guest molecules were then measured in PVA (polyvinyl alcohol). PVA is a kind of water-soluble polymer with a strong ability to construct rigid hydrogen-bonding network and has been widely used to active RTP[32, 33]. The three guests were added into PVA aqueous solution with a very low weight percentage of 0.01% with respect to PVA. After removing water, three transparent films abbreviated by G1@PVA, G2@PVA and G3@PVA were obtained. The three films resemble the above cryogenic methanol solution in photophysical properties. As shown in Fig. 2a, G1@PVA exhibits a dual-emissive PL spectrum, including a fluorescence peak (353 nm, 0.48 ns, Fig. S14a) and a phosphorescence peak (497 nm, 8.74 ms, Fig. 2d). The PL spectra of G2@PVA and G3@PVA are dominated by phosphorescence peaks at 502 nm (8.24 ms) and 508 nm (8.10 ms), respectively (Fig. 2b, 2c and 2d). The triplet energies of the three films are similar with that in diluted methanol solution, which demonstrate that the three guests are fully dispersed in PVA matrix and engender molecular RTP. The absolute phosphorescence quantum yields are 18.0% for G1@PVA, 20.1% for

G2@PVA and 13.5% for G3@PVA respectively (Fig. S15), thereby indicative of relatively similar molecular phosphorescence efficiency.

3.4 The photophysical properties of the three guests in aggregated state at RT

The study on the guest's photophysical properties in aggregated state were also conducted to compare with that in molecular state discussed above. In general, the photophysical properties in aggregated state are very complicated because of too many impact factors, including molecular configuration, packing modes and intermolecular interaction, and as a result, the luminescent properties in aggregated state are generally different from that in molecular state[34, 35]. In our case, G1, G2 and G3 are all fluorescent emitters in aggregated state (420, 415 and 438 nm respectively) and no RTP was detected. (Fig. S16).

3.5 The binding behaviors between phCB[6] and the three guests

Our previous work has revealed an clear 1:1 binding stoichiometry between G1 and phCB[6], therefore G2 and G3 were also expected to form 1:1 complex with phCB[6]. UV-Vis Job's plot method was then carried out to determine the binding stoichiometry between the two guests and the host. When the mole ratio is 1 to 1, the change in absorbance of G2-phCB[6] system reaches a maximum (0.04) with respect to the sole G2, thereby demonstrating a 1:1 stoichiometry (Fig. S17a). G3 and phCB[6] also bind together in 1:1 mole ratio, however, with the maximal change in absorbance (0.03) lowering than that of G2-phCB[6] system (Fig. S17b), which implies a relatively weak binding force. The 1:1 binding mode of G2-phCB[6] and G3-phCB[6] were also confirmed by MALDI-TOF MS measurements, whose results match well with the simulated data (Fig. S18 and S19).

The ^{1}H NMR titration was then conducted to gain more insights into the host-guest binding behaviors. This method has been performed on phCB[6] and G1 in our previous report[30], and the enwrapping degree between them is presented in Scheme 1. The G1 is enwrapped by phCB[6], except for part of benzene ring and the C-Br tail. For G2 and G3, the enwrapping degree would be changed owning to the introduction of methyl substituents. With the help of $^{1}H–^{1}H$ COSY spectra in Fig. S20 and S21, all protons of G2 and G3 can be clearly and properly attributed. As shown in Fig. 3a, proton H_1 and H_2 on G2 both exhibit upfield shift ($\Delta\delta_{H1}$ = -0.54 ppm, $\Delta\delta_{H2}$ = -1.04 ppm), while proton H_4, H_5, H_6 and H_7 all move downfield ($\Delta\delta_{H4}$ = + 0.83 ppm, $\Delta\delta_{H5}$ = + 0.21 ppm, $\Delta\delta_{H6}$ = + 0.14 ppm, $\Delta\delta_{H7}$ = + 0.80 ppm) with the increasing amount of phCB[6]. It is a common rule that the protons inside the hydrophobic cucurbituril cavity undergo shielding effect while the outside ones conduct deshielding effects, and those near the carbonyl rim are scarcely affected[36]. Consequently, it is obviously that the pyridine section and the adjacent methyl are encapsulated by phCB[6], while the remaining moiety locates outside. Proton H_3 is just near the carbonyl portal of phCB[6] owing to its almost unaltered chemical shift. As for G3 in Fig. 3b, all protons show similar change in chemical shifts except for H_3 that exhibits downfield shift ($\Delta\delta_{H3}$ = +

0.19 ppm), which means that only a part of pyridine moiety and adjacent methyl are enwrapped by phCB[6]. Based on the above discussion and the previous work, we conclude that the three guest molecules can all enter into the cavity of phCB[6] in a 1:1 stoichiometry spontaneously in water, however, the enwrapping degrees (G1 > G2 > G3) are various on account of different methyl substitution.

The nonlinear least-squares curve-fitting method[37, 38], which would give more accurate result when compared to the Hildebrand-Benesi equation method, was conducted to determine the host-guest binding constants. The absorption spectra of the three guests in aqueous solution all decrease in intensity gradually with increasing amount of phCB[6], accompanied by bathochromic-shift, thereby further validating the occurrence of host-guest interaction. Three binding constants are determined as 8.5×10^4, 3.1×10^4 and 2.6×10^4 L/mol for phCB[6]/G1, phCB[6]/G2 and phCB[6]/G3 respectively (Fig. 4).

3.6 The photophysical properties of the host-guest complexes in solid state

The three guests and phCB[6] were then mixed respectively in 1:1 mole ratio in water (0.1 mmol in 4 mL) and three white powders were obtained after lyophilization, which are denoted as phCB[6]/G1, phCB[6]/G2 and phCB[6]/G3 respectively. The ^{1}H NMR of the three complexes with clear protons attribution are listed in Fig. S22-S24. The PL spectrum of phCB[6]/G1 is occupied by a phosphorescence peak (526 nm, 10.2 ms, Fig. 4a and 4d), accompanying with a small fluorescence peak (394 nm, 0.45 ns, Fig. 4a and Fig. S25), while those of phCB[6]/G2 and phCB[6]/G3 are dominated by phosphorescence peaks (522 nm, 4.8 ms and 524 nm, 5.9 ms, as shown in Fig. 4b, 4c and 4d). The three PL spectra are relatively similar to those of G1, G2 and G3 in cryogenic methanol or in PVA films, which is reasonable because phCB[6] provides an individual microenvironment for every guest molecular to avoid possible intermolecular interaction. Under the excitation of 365 nm lamp, the three powders all emit yellow-green light, and phCB[6]/G1 is more brilliant than phCB[6]/G2 and phCB[6]/G3 by naked eyes, implying a higher phosphorescence efficiency. The obtained absolute phosphorescence quantum yields are 78%, 36% and 18%, respectively (Fig. S26), showing obvious dependence on the binding behaviors between host and guest - the higher enwrapping degree, the higher RTP efficiency. It is rational that higher enwrapping degree would result in stronger restraint of molecular motion and more effective shielding of oxygen, high RTP performance thus originates. The phosphorescence properties involved in this work are summarized and listed in Table 1.

Table 1
The phosphorescence properties involved in this work

	λ_{phos} (nm)	τ_{phos} (ms)	Φ_{phos} (%)	K (10^4 L/mol)
G1 in 77 K	495	20.1		
G2 in 77 K	500	18.5		
G3 in 77 K	500	18.0		
G1@PVA	497	8.74	18.0	
G2@PVA	502	8.24	20.1	
G3@PVA	508	8.10	13.5	
phCB[6]/G1	526	10.2	78.0	8.6
phCB[6]/G2	522	4.80	36.0	3.1
phCB[6]/G3	524	5.90	18.0	2.6

4. Conclusion

In this work, three guest compounds G1, G2 and G3 with a same luminescent core (4-(4-bromophenyl)-1-methylpyridinium chloride) and different number of methyl substituents were designed and synthesized. These guests show similar phosphorescence emission maximum (approximate 500 nm) and phosphorescence yield (18.0% for G1, 20.1% for G2 and 13.5% for G3 respectively) in molecular state. When assembled respectively with phCB[6], three 1:1 host-guest complexes phCB[6]/G1, phCB[6]/G2 and phCB[6]/G3 were obtained with different enwrapping degrees. Due to the steric hindrance from the increasing number of methyl, the entry depth of guests into the cavity of phCB[6] decrease gradually from benzene moiety for G1 to pyridine moiety for G2, and last to the N cation for G3, thereby showing an obvious descending trend of enwrapping degrees. The absolute RTP quantum yields of phCB[6]/G1, phCB[6]/G2 and phCB[6]/G3 are 78%, 36% and 18% respectively, which obviously demonstrate that the enwrapping degrees between host and guest plays an important role in supramolecular RTP performance. To our knowledge, this is the first report about the relationship between supramolecular phosphorescence performance and host-guest binding behaviors. This work may provide a new design idea for preparing high-performed supramolecular RTP materials.

Declarations

Acknowledgement This work was financially supported by Shanghai Municipal Science and Technology Major Project (No. 2018SHZDZX03), National Natural Science Foundation of China (Nos. 21788102, 21572063), and the Fundamental Research Funds for the Central Universities.

Competing interests The authors declare no competing interests.

Confict of interests The authors declare that they have no known competing fnancial interests or personal relationships that could have appeared to infuence the work reported in this paper.

Ethical approval This article does not involve any animal experiment or human subject experiment.

Availability of data and materials The datasets generated and/or analyzed in the course of the current

study are available from the corresponding author on reasonable request.

Authors' contributions Chunhui Li and Qichao Guo were involved in experimental research, writing original draft, formal analysis, validation. Jinkang Zhu helped in experimental research. Qiaochun Wang conceived, planned and supervised this work.

Funding This work was financially supported by Shanghai Municipal Science and Technology Major Project (No. 2018SHZDZX03), National Natural Science Foundation of China (Nos. 21788102, 21572063), and the Fundamental Research Funds for the Central Universities.

References

1. Y. Su, Y. Zhang, Z. Wang, W. Gao, P. Jia, D. Zhang, C. Yang, Y. Li and Y. Zhao, Angew. Chem. Int. Ed. **59**, 25 (2020)
2. Y. Wang, H. Gao, J. Yang, M. Fang, D. Ding, B.Z. Tang and Z. Li, Adv. Mater. **33**, 18 (2021)
3. W. Ye, H. Ma, H. Shi, H. Wang, A. Lv, L. Bian, M. Zhang, C. Ma, K. Ling, M. Gu, Y. Mao, X. Yao, C. Gao, K. Shen, W. Jia, J. Zhi, S. Cai, Z. Song, J. Li, Y. Zhang, S. Lu, K. Liu, C. Dong, Q. Wang, Y. Zhou, W. Yao, Y. Zhang, H. Zhang, Z. Zhang, X. Hang, Z. An, X. Liu and W. Huang, Nat. Mater. **20**, 11 (2021)
4. S. Sun, J. Wang, L. Ma, X. Ma and H. Tian, Angew. Chem. Int. Ed. **60**, 34 (2021)
5. S. Wang, H. Shu, X. Han, X. Wu, H. Tong and L. Wang, J. Mater. Chem. C **9**, 31 (2021)
6. B. Ding and X. Ma, Langmuir **37**, 49 (2021)
7. Z. An, C. Zheng, Y. Tao, R. Chen, H. Shi, T. Chen, ZhixiangWang, H. Li, R. Deng, X. Liu and W. Huang, Nat. Mater. **14**, 7 (2015)
8. Z. Yang, C. Xu, W. Li, Z. Mao, X. Ge, Q. Huang, H. Deng, J. Zhao, F.L. Gu, Y. Zhang and Z. Chi, Angew. Chem. Int. Ed. **59**, 40 (2020)
9. J. Chen, X. Chen, L. Cao, H. Deng, Z. Chi and B. Liu, Angew. Chem. Int. Ed. **61**, 24 (2022)
10. Z. Yang, Z. Mao, X. Zhang, D. Ou, Y. Mu, Y. Zhang, C. Zhao, S. Liu, Z. Chi, J. Xu, Y.C. Wu, P.Y. Lu, A. Lien and M.R. Bryce, Angew. Chem. Int. Ed. **55**, 6 (2016)
11. B. Ding, L. Ma, Z. Huang, X. Ma and H. Tian, Sci. Adv. **7**, 19 (2021)
12. S. Garain, S.N. Ansari, A.A. Kongasseri, B. Chandra Garain, S.K. Pati and S.J. George, Chem. Sci. **13**, 34 (2022)
13. Y. Lei, W. Dai, J. Guan, S. Guo, F. Ren, Y. Zhou, J. Shi, B. Tong, Z. Cai, J. Zheng and Y. Dong, Angew. Chem. Int. Ed. **59**, 37 (2020)

14. S. Garain, A.K. Singh, S.C. Peter and S.J. George, Mater. Res. Bull. **142**, (2021)
15. L. Gu, H. Wu, H. Ma, W. Ye, W. Jia, H. Wang, H. Chen, N. Zhang, D. Wang, C. Qian, Z. An, W. Huang and Y. Zhao, Nat. Commun. **11**, 1 (2020)
16. L. Gu, W. Ye, X. Liang, A. Lv, H. Ma, M. Singh, W. Jia, Z. Shen, Y. Guo, Y. Gao, H. Chen, D. Wang, Y. Wu, J. Liu, H. Wang, Y.X. Zheng, Z. An, W. Huang and Y. Zhao, J. Am. Chem. Soc. **143**, 44 (2021)
17. S. Garain, B.C. Garain, M. Eswaramoorthy, S.K. Pati and S.J. George, Angew. Chem. Int. Ed. **60**, 36 (2021)
18. Z. Qian, T. Yuan and Q. Wang, Res. Chem. Intermed. **44**, 10 (2018)
19. T. Yuan, W. Gao and Q. Wang, Res. Chem. Intermed. **48**, 1 (2022)
20. H.J. Yu, X.L. Zhou, X. Dai, F.F. Shen, Q. Zhou, Y.M. Zhang, X. Xu and Y. Liu, Chem. Sci. **13**, 27 (2022)
21. J. Wang, Z. Huang, X. Ma and H. Tian, Angew. Chem. Int. Ed. **59**, 25 (2020)
22. X.K. Ma and Y. Liu, Acc. Chem. Res. **54**, 17 (2021)
23. M. Huo, X.Y. Dai and Y. Liu, Adv. Sci. **9**, 22 (2022)
24. X.K. Ma, X. Zhou, J. Wu, F.F. Shen and Y. Liu, Adv. Sci. **9**, 18 (2022)
25. C. Wang, Y.H. Liu and Y. Liu, Small **18**, 21 (2022)
26. D.-A. Xu, Q.-Y. Zhou, X. Dai, X.-K. Ma, Y.-M. Zhang, X. Xu and Y. Liu, Chin. Chem. Lett. **33**, 2 (2022)
27. W.-L. Zhou, W. Lin, Y. Chen, X.-Y. Dai, Z. Liu and Y. Liu, Chem. Sci. **13**, 2 (2022)
28. X.Y. Dai, M. Huo, X. Dong, Y.Y. Hu and Y. Liu, Adv. Mater. **34**, 38 (2022)
29. D. Lucas, T. Minami, G. Iannuzzi, L. Cao, P. Anzenbacher, Jr. and L. Isaacs, J. Am. Chem. Soc. **133**, 44 (2011)
30. C. Li, X. Li and Q. Wang, Chin. Chem. Letter. **33**, 2 (2022)
31. W. Dai, X. Niu, X. Wu, Y. Ren, Y. Zhang, G. Li, H. Su, Y. Lei, J. Xiao, J. Shi, B. Tong, Z. Cai and Y. Dong, Angew. Chem. Int. Ed. **61**, 13 (2022)
32. Y. Su, S.Z.F. Phua, Y. Li, X. Zhou, D. Jana, G. Liu, W.Q. Lim, W.K. Ong, C. Yang and Y. Zhao, Sci. Adv. **4**, 5 (2018)
33. H. Wu, W. Chi, Z. Chen, G. Liu, L. Gu, A.K. Bindra, G. Yang, X. Liu and Y. Zhao, Adv. Funct. Mater. **29**, 10 (2018)
34. S. Li, L. Fu, X. Xiao, H. Geng, Q. Liao, Y. Liao and H. Fu, Angew. Chem. Int. Ed. **60**, 33 (2021)
35. J. Zhu, Q. Liao, H. Huang, L. Fu, M. Liu, C. Gu and H. Fu, Cell Reports Physical Science **3**, 1 (2022)
36. H. Zhang, Q. Wang, M. Liu, X. Ma and H. Tian, Org. Lett. **11**, 15 (2009)
37. F.F. Shen, Y. Chen, X. Dai, H.Y. Zhang, B. Zhang, Y. Liu and Y. Liu, Chem. Sci. **12**, 5 (2021)
38. X.K. Ma, Y.M. Zhang, Q. Yu, H. Zhang, Z. Zhang and Y. Liu, Chem. Commun. **57**, 10 (2021)

Schemes

Schemes are available in Supplementary Files section.

Figures

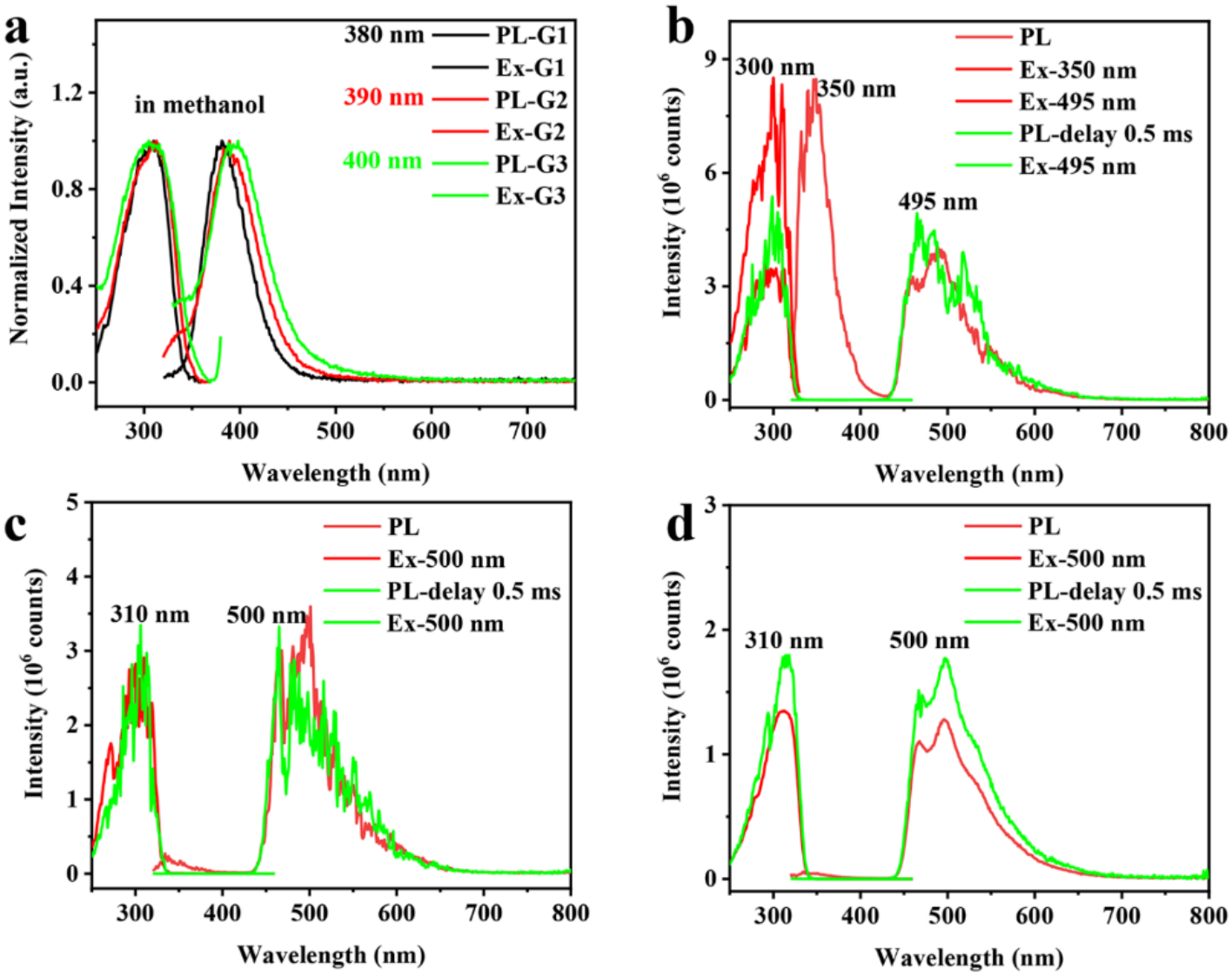

Figure 1

a) The normalized PL and excitation spectra of the three guests in methanol at RT. The PL and delayed PL spectra of b) G1, c) G2 and d) G3 in methanol at 77 K.

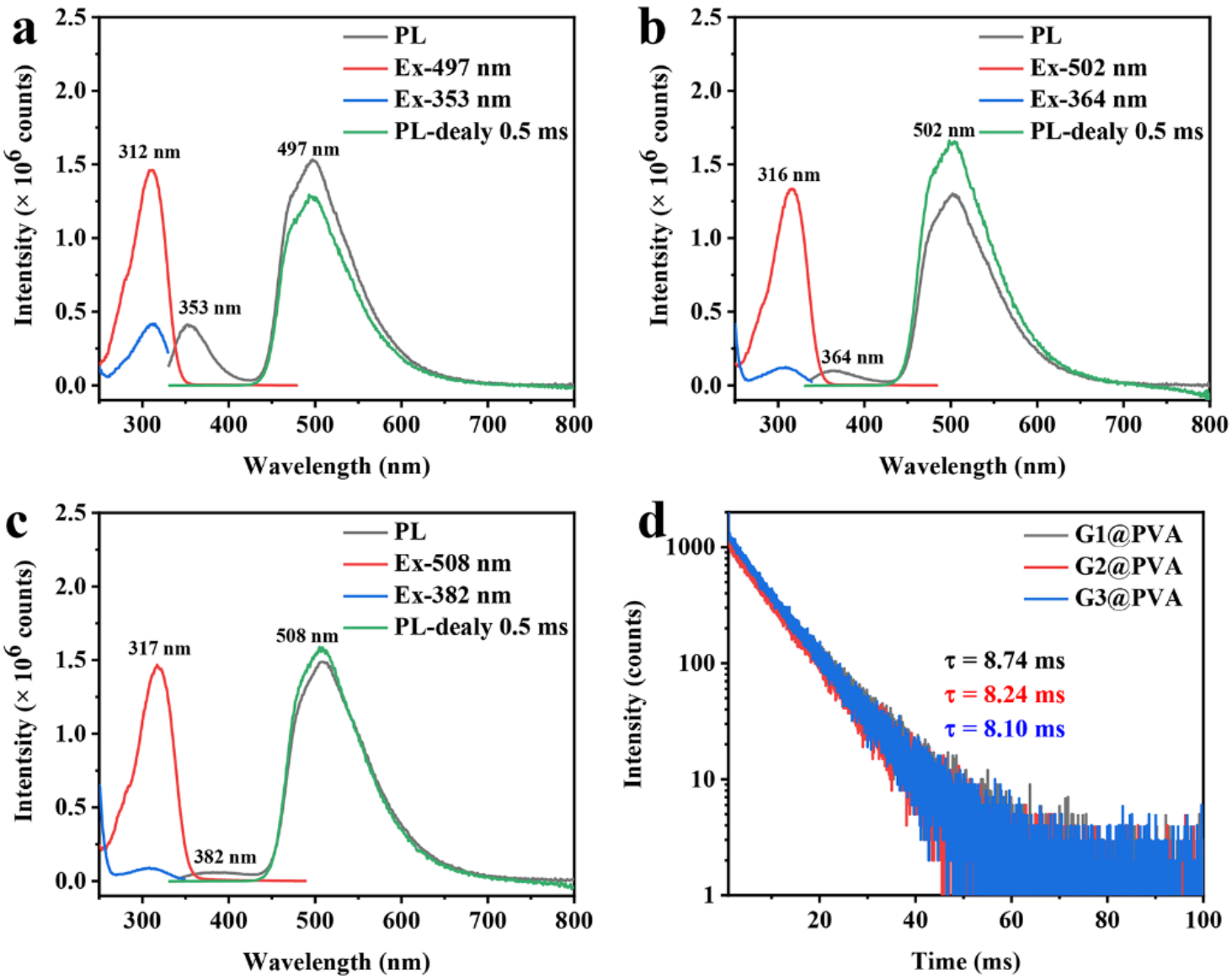

Figure 2

The PL, delayed PL and corresponding excitation spectra of a) G1@PVA, b) G2@PVA and c) G3@PVA. d) Phosphorescence life decay curves for the three films.

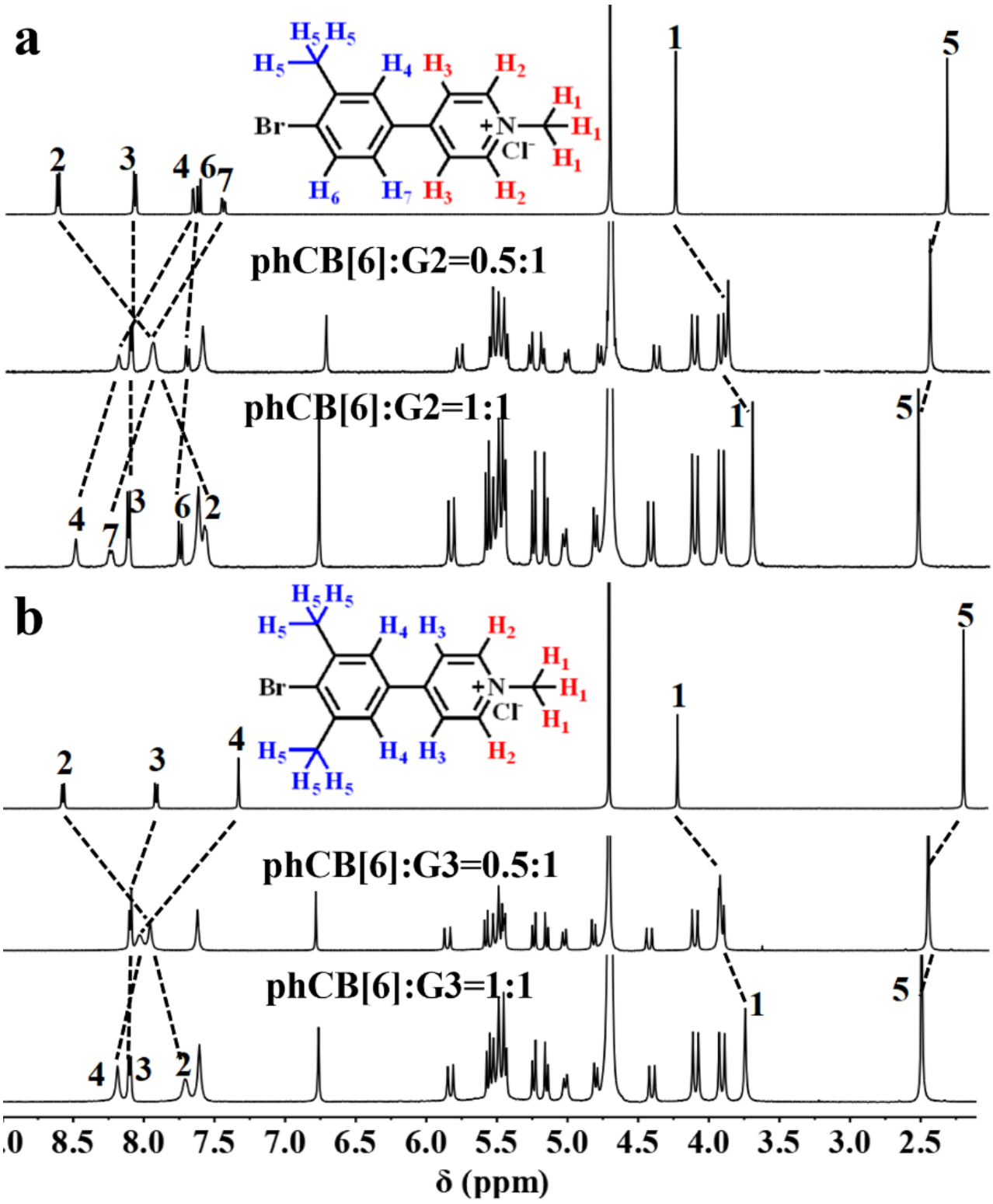

Figure 3

Titration of phCB[6] into a) G2 and b) G3 monitored in D_2O by ^1H NMR spectroscopy at 298 K. The red protons represent a shielding effect and the bule protons show a deshielding effect.

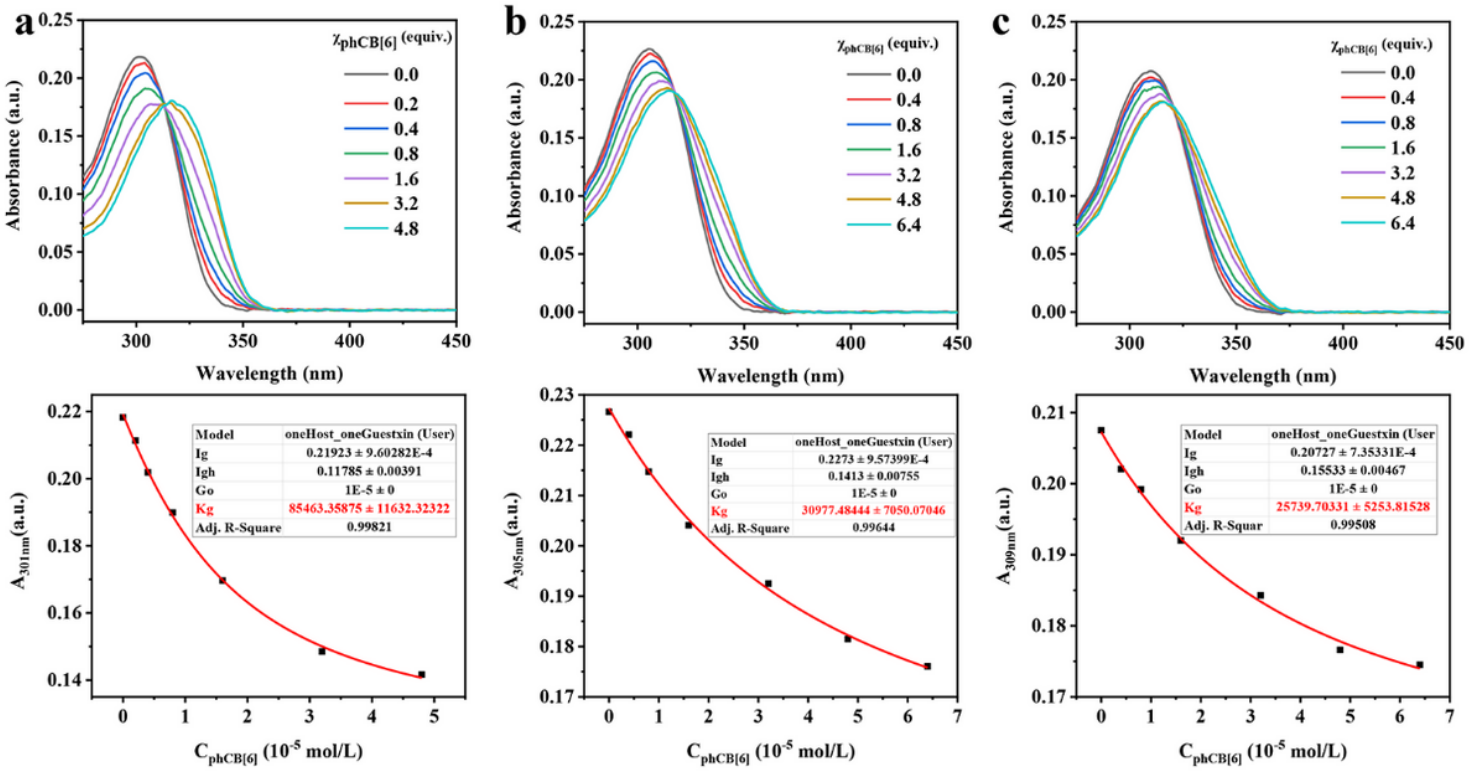

Figure 4

UV-vis absorption spectra of a) G1, b) G2, c) G3 at a concentration of 1×10^{-5} mol/L in aqueous solution upon the gradual addition of phCB[6] and the corresponding binding constants (K_g) fitted by the nonlinear least squares curve-fitting method.

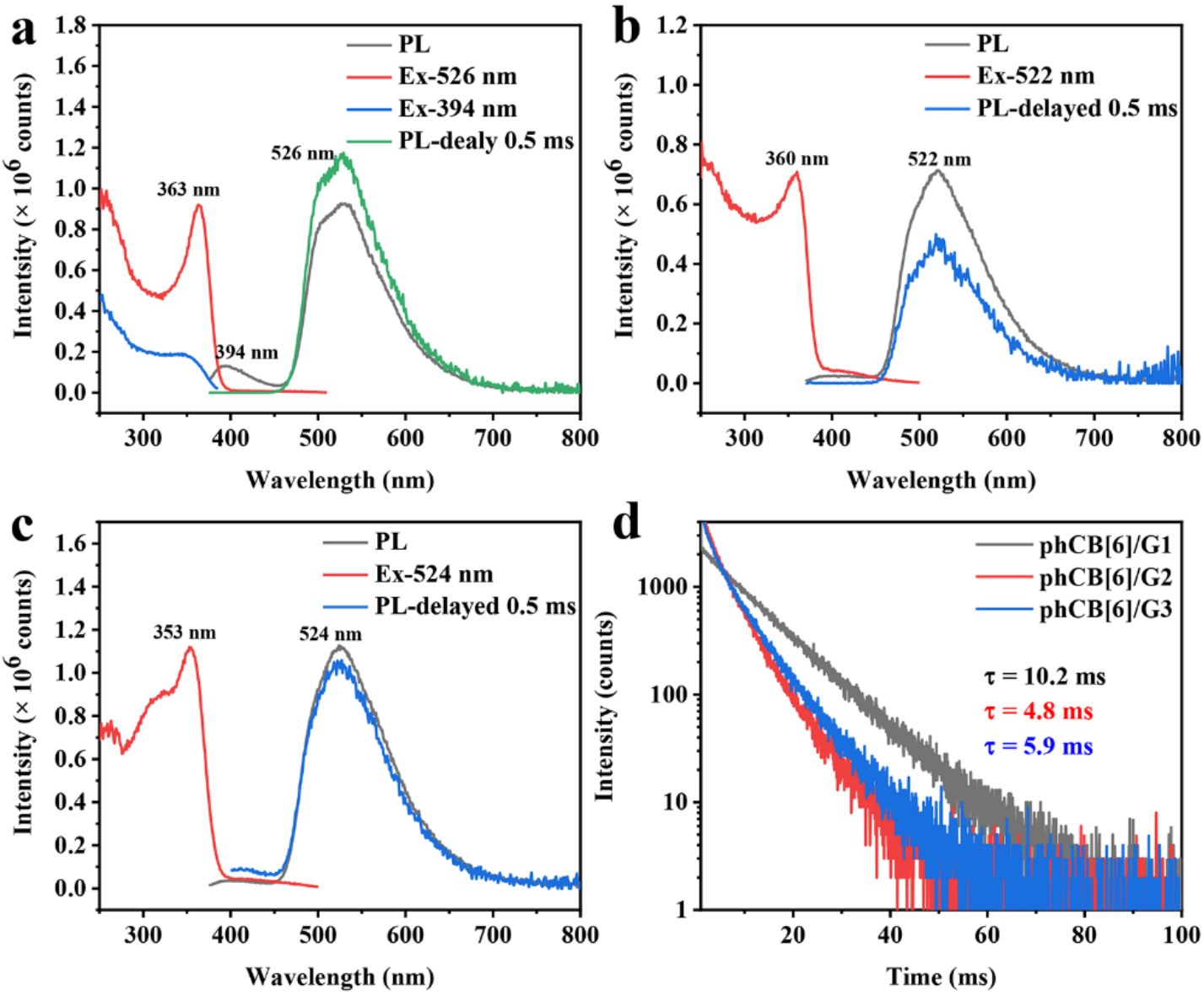

Figure 5

The PL, delayed PL and corresponding excitation spectra of a) phCB[6]/G1, b) phCB[6]/G2 and c) phCB[6]/G3. d) Phosphorescence life decay curve for the three complexes.

Supplementary Files

This is a list of supplementary files associated with this preprint. Click to download.

- Scheme1.png
- Scheme2.png
- Supportinginformation.docx